Dalton Transactions

PAPER

View Article Online
View Journal | View Issue

Check for updates

Cite this: *Dalton Trans.*, 2019, **48**, 17083

Ferrocenyl palladacycles derived from unsymmetrical pincer-type ligands: evidence of Pd(0) nanoparticle generation during the Suzuki–Miyaura reaction and applications in the direct arylation of thiazoles and isoxazoles†

Ankur Maji,[a] Anshu Singh,[a] Aurobinda Mohanty,[a] Pradip K. Maji *[b] and Kaushik Ghosh *[a]

Received 26th August 2019,
Accepted 16th October 2019

DOI: 10.1039/c9dt03465j

rsc.li/dalton

A new family of ferrocenyl-palladacycle complexes Pd(L^1)Cl (**Pd1**) and Pd(L^2)Cl (**Pd2**) were synthesized and characterized by UV-visible, IR, ESI-MS, and NMR spectral studies. The molecular structures of **Pd1** and **Pd2** were determined by X-ray crystallographic studies. Palladacycle catalyzed Suzuki–Miyaura cross-coupling reactions were investigated utilizing the derivatives of phenylboronic acids and substituted chlorobenzenes. Mechanistic investigation authenticated the generation of Pd(0) nanoparticles during the catalytic cycle and the nanoparticles were characterized by XPS, SEM and TEM analysis. Direct C–H arylation of thiazole and isoxazole derivatives employing these ferrocenyl-palladacycle complexes was examined. The reaction model for the arylation reaction implicating the *in situ* generation of Pd(0) nanoparticles was proposed.

Introduction

Over the past few decades, ferrocene has been the most employed metallocene due to its unique electrochemical properties and its applications in medicinal chemistry.[1] On the other hand, ferrocene-based co-ordination complexes have been utilized for molecular recognition and as cytotoxic agents.[2] Cyclometalated organometallic complexes based on 6-phenyl-2,2′-bipyridine (NNC) have been widely utilized for their catalytic and luminescence properties.[3] Reports on ferrocenyl based NNC ligands and their metal complexes are scarce in the literature; however, ferrocene based ligands having a combination of phosphorus, nitrogen and sulfur are known.[4] The presence of a Pd–C σ-bond as the central or exterior donor site plays a significant role in thermal stability, potential hemilability and catalytic activity.[5] Along the same lines, the use of the palladacycles of ligands having (N,N) donor groups present in an arm of ferrocene is limited and, to the best of our knowledge, their catalytic applications have not been reported in the literature.[6]

In fact, this class of ligands were utilized for the chelation assisted C–H bond functionalization of the C2 position of ferrocene derivatives.[7] Several transition metals like Ir, Rh, and Pd have been used for the activation of the C2–H of the ferrocene moiety and for the synthesis of ferrocene derivatives.[8]

The Suzuki–Miyaura cross-coupling (SMC) reaction is the traditional method for C–C bond formation. Palladium complexes derived from phosphine-based ligands are the conventional ligands for the SMC coupling reaction.[9] At present organometallic pincer type (NNC or NCN) palladium(II) complexes with different types of donor atoms are widely employed as catalysts for coupling reactions.[10] The use of ferrocene based organometallic complexes in such cross-coupling reactions is less explored yet.[11] Though the SMC reactions of aryl bromides and iodides are available, reports on aryl chlorides are not abundant due to the difficulty in the activation of C–Cl bonds compared to C–Br or C–I bonds with low catalyst loading (0.0001 mol%).[12]

Compared to well-recognized traditional cross-coupling reactions, the palladium-catalyzed direct arylation *via* C–H

[a]*Department of Chemistry, Indian Institute of Technology Roorkee, Roorkee 247667, Uttarakhand, India. E-mail: ghoshfcy@iitr.ernet.in; Fax: +91-1332-273560; Tel: +91-1332-275547*

[b]*Department of Polymer and Process Engineering, Indian Institute of Technology Roorkee, Saharanpur Campus, Saharanpur, UP 247001, India. E-mail: pradip.fpt@iitr.ac.in*

†Electronic supplementary information (ESI) available: Experimental section, NMR, MS, and UV-visible spectral data and information on DFT calculations. X-ray crystal structure data have been deposited in the Cambridge Crystallographic Data Centre and the deposition number for complex **Pd1** is CCDC 1939017 and for complex **Pd2** is CCDC 1939018. For ESI and crystallographic data in CIF or other electronic format see DOI: 10.1039/C9DT03465J

bond activation is observed to be more reliable and environmentally friendly.[13] Direct arylation of isoxazoles and thiazoles provides important molecules having potential use in medicinal chemistry.[14] The function of supporting ligands in such arylation reactions has been proved to play a significant role during the catalytic process. Among the ligands reviewed, it is important to note that phosphine-free ligands, particularly nitrogen-based ligands, have generated considerable interest due to their air stability and high catalytic performance. In the literature 1,10-phenanthroline (phen)/$Pd(OAc)_2$ could efficiently catalyze the direct C–H arylation reaction of imidazoles with aryl halides to give regioselective products.[15] Palladium complexes derived from nitrogen-based ligands facilitate reductive elimination steps in direct arylation reactions.[14] Moreover, organometallic palladium complexes could not only facilitate reductive elimination steps but also generate Pd(0) nanoparticles during the catalytic reactions.[16] Very few reports have described direct arylation *via* sp^2 (C–H) bond activation catalyzed by *in situ* generated Pd(0) nanoparticles.[17]

In the present study, we have designed and synthesized ferrocene-based organometallic palladium complexes. We would like to mention here that the iron atom in the metalloligands containing ferrocene arms decreases their donor and/or increases their acceptor properties, which in turn causes a change in the catalytic activity of the C-coordinated Pd complexes.[11,16b] These complexes were utilized for SMC cross-coupling reactions. During our investigation of the mechanism of the catalytic process, the generation of Pd(0) nanoparticles was indicated. *In situ* generated Pd(0) nanoparticles were analyzed by field-emission scanning electron microscopy (FE-SEM), transmission electron microscopy (TEM) and X-ray photoelectron spectroscopy (XPS). We have investigated direct arylation *via* sp^2 (C–H) bond activation and performed arylation reactions of isoxazoles and thiazoles with different aryl halides.

Results and discussion

Synthesis of ligands

Ligands (**L1H** and **L2H**) were synthesized by the condensation of ferrocenecarboxaldehyde, 2-(1-phenylhydrazinyl)pyridine[18] and 2-((1-phenylhydrazinyl)methyl)pyridine[19] in an equimolar ratio respectively. After 3 hours deep red colored precipitates of ligands **L1H** and **L2H** were obtained and characterized by UV-visible, IR and NMR spectroscopy. The ^{1}H-NMR spectra of **L1H** and **L2H** showed one doublet at around ~8.0 ppm due to the adjacent proton of pyridine[18,19] and for **L2H** one singlet was observed at ~4.0 ppm due to the presence of the $-CH_2-$ proton.[16] The ^{1}H-NMR peaks confirmed the formation of Schiff bases **L1H** and **L2H**, respectively. The ESI-mass spectral study was performed for both the ligands in the acetonitrile solution. Ligands **L1H** and **L2H** showed peaks at m/z = 382.0305 (for the $[\mathbf{L1H}]^+$ ion) and m/z = 395.1137 (for the $[\mathbf{L2H}]^+$ ion) respectively which authenticate the formation of Schiff bases (spectra are shown in ESI Fig. S15 and S16†).

Synthesis of palladacycles

Palladium complexes $Pd(L^1)Cl$ (**Pd1**) and $Pd(L^2)Cl$ (**Pd2**) were synthesized using the $Na_2[PdCl_4]$ metal salt and neutral ligands $\mathbf{L^1H}$ and $\mathbf{L^2H}$ in an equimolar ratio in methanol (shown in Scheme 1). Coordination of ligands with the metal was analyzed primarily based on UV-visible, IR, and NMR spectral studies. The absorption spectra of all the complexes were recorded in dichloromethane at room temperature (Table S1 and Fig. S1†). The absorption bands of $\mathbf{L^1H}$ near 332, 290 and 251 nm were assigned to n → π* and π → π* transitions of the ligand. The absorption band of $\mathbf{L^1H}$ near 484 nm was assigned to ligand-to-metal (iron) charge transfer (LMCT) transitions.[20] Complex **Pd1** showed a broad band near 532 nm due to ligand to metal (palladium) charge transfer (LMCT) transitions (shown in Fig. S1†). In the case of $\mathbf{L^2H}$, the peaks near 255 and 325 nm were assigned to intra-ligand n → π* and π → π* transitions and that at 435 nm was assigned to ligand to metal (iron) charge transfer transitions. Complex **Pd2** showed a broad band near 535 nm due to the ligand to metal (palladium) charge transfer (LMCT) transition (Fig. S1†).[20] During IR spectral studies coordination of nitrogen to the metal center resulted in a shift in $\nu_{(-HC=N)}$. For complex **Pd1** the stretching frequency of the $\nu_{(-HC=N)}$ shift was around 35 cm^{-1} and for complex **Pd2** a shift of 10 cm^{-1} was observed (shown in Fig. S2–S5†).[20] The complexes are diamagnetic and displayed well-resolved ^{1}H-NMR and ^{13}C-NMR spectra in d^6-DMSO solution (shown in ESI Fig. S8–S12†). The ^{1}H-NMR signal of the imine of **Pd1** was shifted from ~7.07 ppm to ~7.10 ppm and for **Pd2** the doublet proton of pyridine hydrogen shifted from ~8.68 to 9.06 ppm due to complexation.[19] The ^{1}H-NMR signal of the $-CH_2-$ singlet proton shifted from

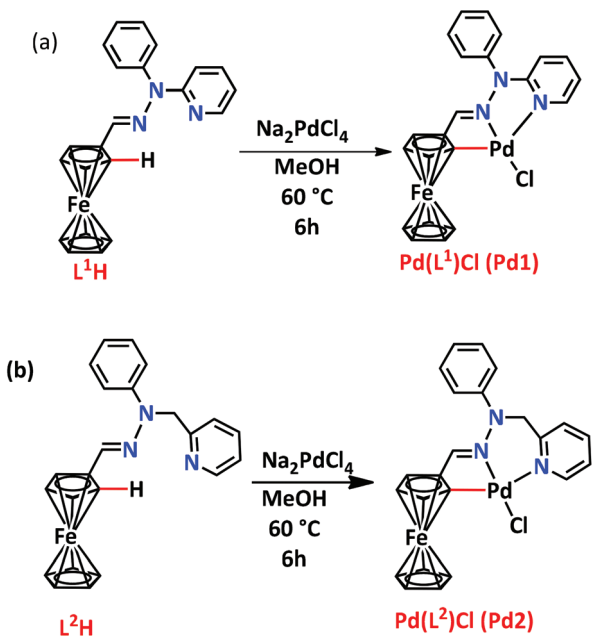

Scheme 1 Schematic representation of synthesized complexes **Pd1** (a) and **Pd2** (b).

5.22 ppm to 5.75 ppm due to the metal–ligand coordination of **Pd2**. In the NMR spectral splitting of ferrocene, protons were observed due to carbon–metal bond formation.[17] ESI-MS analysis of **Pd1** and **Pd2** was performed in the acetonitrile solution and *m*/*z* peaks at 527.0384 [**Pd1** + CH_3CN–Cl]$^+$ for **Pd1** and at 534.9662 [**Pd2** + H^-]$^+$ for **Pd2** were recorded. Spectra are shown in ESI Fig. S14–S16.†

Crystal structures of Pd1 and Pd2

The single crystals of **Pd1** and **Pd2** suitable for X-ray diffraction were grown by slow evaporation in a dichloromethane and methanol (1 : 3) mixture. The crystal structure data and refinement parameters for complexes **Pd1** and **Pd2** are given in ESI Table S2.† Selected bond distances and bond angles are shown in ESI Tables S3 and S4.† The ORTEP diagrams (30% probability of ellipsoids) of complexes **Pd1** and **Pd2** are shown in Fig. 1 and 2. The Pd(1)–N(1) bond lengths of **Pd1** and **Pd2** are 2.125(5) and 2.155(4) Å respectively which are higher than those reported in our previous report,[19c] however, consistent with those reported by Sokolov and co-workers.[21] The

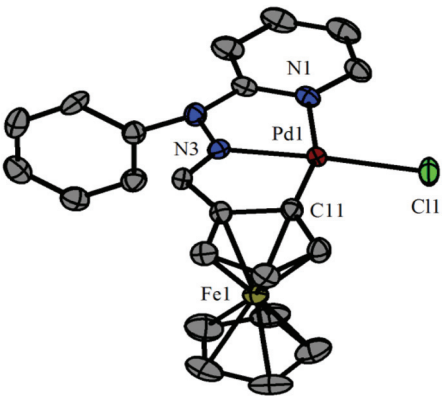

Fig. 1 The ORTEP diagram (30% probability level) of complex **Pd1**. Hydrogen atoms are omitted for clarity.

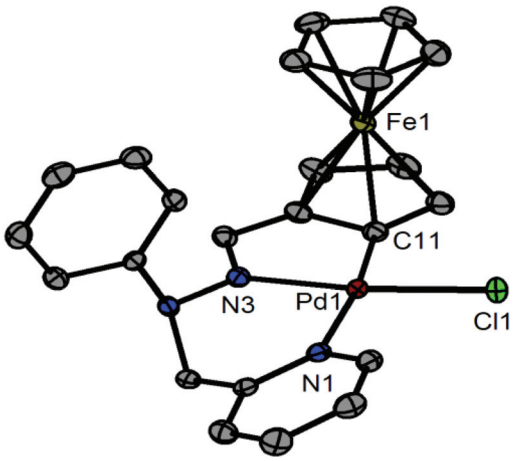

Fig. 2 The ORTEP diagram (30% probability level) of complex **Pd2**. Hydrogen atoms are omitted for clarity of the structure.

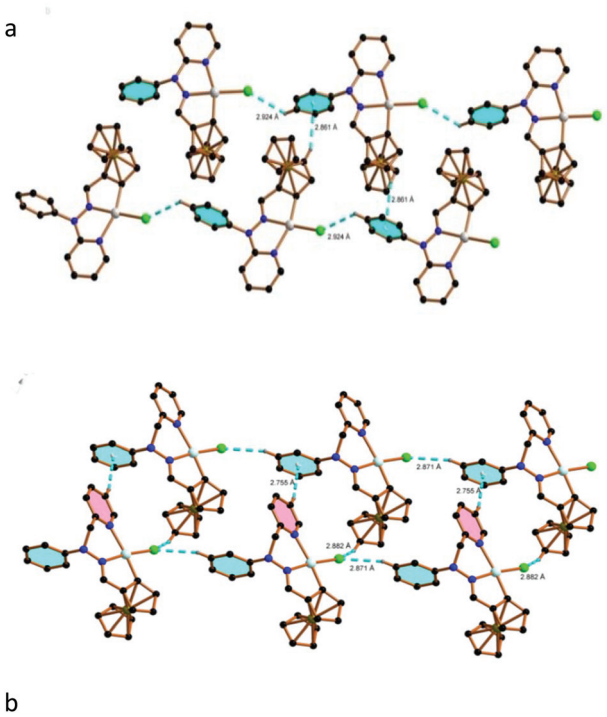

Fig. 3 Ball-and-stick representation of intermolecular halogen-bonding and C–H···π interaction in infinite chains. Hydrogen atoms are omitted for clarity. Color code: carbon, black; nitrogen, blue; chlorine, light green, Pd, white; and XBs: dotted greenish-blue.

Pd(1)–N(3) bond distances of **Pd1** and **Pd2** are 1.986(5)(Å) and 2.015(6) (Å), respectively, which are higher than the literature values.[16b,19c] The Pd(1)–C(11) bond lengths of **Pd1** and **Pd2** are 1.968(6) and 1.972(4) Å respectively which are consistent with those reported by Singh and co-workers and Sokolov and co-workers.[16b,21] The N3–**Pd1**–Cl1 and C11–**Pd1**–N1 bond angles of complex **Pd1** are 176.48(15)° and 160.27(22)° respectively which show distorted square planar geometry and are in good agreement with theoretical values. C–H···Cl secondary interactions result in the formation of chains as shown in Fig. 3.

Suzuki–Miyaura reaction

The catalytic activity of complexes **Pd1** and **Pd2** was examined towards the Suzuki–Miyaura reactions of aryl chloride derivatives with phenylboronic acids. Reports to date on palladacycles as powerful catalysts for Suzuki–Miyaura reactions have mainly focused on phosphorus, sulfur, nitrogen and selenium-containing structures, including N-heterocyclic carbene (NHC) compounds.[16b,21–24] With **Pd1** as the precatalyst, the coupling reaction between 4-chlorobenzaldehyde (**1a**) and phenylboronic acid (**2a**) chosen as the model reaction is shown in Scheme 2. After careful optimization of the reaction conditions [1,1′-biphenyl]-4-carbaldehyde (**3**) was isolated and its yield was 95% in DMF : H_2O (2 : 1) at 80 °C when K_2CO_3 was utilized as the base as shown in Scheme 2 and Table 1.

Initially, the catalytic reactions studied with various bases such as KOH, NaOH, K_2CO_3, Na_2CO_3, CH_3COONa, K^{t}OBu and

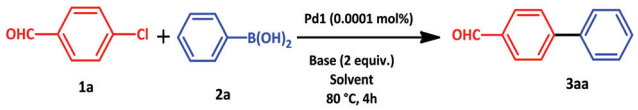

Scheme 2 Reaction optimization for the Pd-catalyzed Suzuki–Miyaura reaction.

Table 1 Optimization of solvents and bases in the presence of **Pd1**

Entry	Base	Solvent	%Yield
1	K_2CO_3	Toluene : water (2 : 1)	81
2	K_2CO_3	Ethanol : water (2 : 1)	78
3	K_2CO_3	Water	25
4	K_2CO_3	DMF : water (2 : 1)	95
5	K_2CO_3	DMSO : water(2 : 1)	91
6	K_2CO_3	Benzene : water (2 : 1)	82
7	K_2CO_3	NMP : water	89
8	KOH	DMF : water (2 : 1)	61
9	NaOH	DMF : water (2 : 1)	65
10	Na_2CO_3	DMF : water (2 : 1)	95
11	NaOAc	DMF : water (2 : 1)	74
12	KOAc	DMF : water (2 : 1)	75
13	K_3PO_4	DMF : water (2 : 1)	65
14	$NaHCO_3$	DMF : water (2 : 1)	55
15	K^tOBu	DMF : water (2 : 1)	59
16	Et_3N	DMF : water (2 : 1)	74
17	K_2CO_3	DMF : water (2 : 1)	NR[a]
18	K_2CO_3	DMF : water (2 : 1)	NR[b]

Reaction conditions: **Pd1** (0.0001 mol%), **2a** (1.0 mmol), **3a** (1.2 mmol), base (2 mmol), solvent (4.5 mL), 80 °C, 4 h. [a] Only the ligand (0.01 mol%). [b] Only in the presence of (0.01 mol%) $Na_2[PdCl_4]$.

Et_3N, where K_2CO_3 and Na_2CO_3 provided a coupled product in a yield of 95% (isolated yield), are summarized in Table 1. The SMC reaction was very limited in neat water due to the insolubility of the catalyst (Table 2, entry 3). This problem was overcome by adding organic solvents to dissolve the catalyst in the reaction medium. Control experiments revealed that the SMC reaction does not proceed in the presence of only ligand ($\mathbf{L^1H}$) (Table 1, entry 17). Commonly available $Na_2[PdCl_4]$ was also found to be ineffective (Table 1, entry 18).

We further scrutinized the substrate scope of the reactions of various haloarenes with organoboronic acids in the presence of complexes **Pd1** and **Pd2**. The reactions gave good results for activated aryl chlorides (Table 2), and the TON was up to 95×10^4 (Table 2, **3aa–3ae** and **3al–3ap**). Unactivated hetero-chloroarenes also worked using complexes **Pd1** and **Pd2** but with moderate yields of up to 65% to 78% (Table 2, **3af–3ah**, **3aq–3as**, **3au** and **3av**). These catalysts were also utilized for the sequential cross-coupling reaction of 2,6-dichloropyridine which afforded 2,6-diphenylpyridine and 2,6-bis(4-ethylphenyl)pyridine in moderate yields of 65%–71% (Table 2, **3ah** and **3as**). Sterically hindered 1-naphthyl chloride resulted in yields of 85% to 91% (Table 2, **3ak** and **3at**).

We next explored the substrate scope of the reactions of the electron-withdrawing phenylboronic acids (4-Cl and 4-F) with different haloarenes in the presence of complexes **Pd1** and **Pd2**. Both electron-withdrawing phenylboronic acids (4-Cl and 4-F) react with 4-$COCH_3$ and 4-CN chlorobenzenes to give products in very good to excellent yields (Table 2, **3ba**, **3bb**, **3ca** and **3cb**). The reactions of heteroarenes 3-chloropyridine and 2-chloroquinoline with (4-Cl and 4-F) phenylboronic acids also provided cross-coupled products in very good to excellent yields (Table 2, **3bc**, **3bd**, **3cc** and **3cd**). Interestingly, 3-NO_2 chlorobenzene smoothly coupled with (4-Cl and 4-F) phenylboronic acids to give products in excellent yields (Table 2, **3be** and **3ce**). Both electron-withdrawing phenylboronic acids (4-Cl and 4-F) react with 2-NO_2 chlorobenzene to give products in moderate yields (Table 2, **3bf** and **3cf**).

According to the literature, the best results for coupling of aryl chlorides were achieved with palladium complexes derived from phosphorus-containing pincer complexes or with palladacycles modified with carbenes.[11,21–23] Our results are comparable with the data reported by Richards and coworkers.[11a] Nevertheless our catalysts are more active than other catalysts reported in the literature.[21,23,24]

Probable reaction pathway

During SMC reactions catalyzed by **Pd1** and **Pd2**, the solution turned black immediately after mixing the reactants.[16] We accomplished several experiments to recognize the catalytically active species in our reaction. We speculate that the active catalytic species was not the complex, but rather some *in situ* generated species in the reaction mixture. We performed X-ray photoelectron spectroscopic (XPS) analysis for investigating the surface compositions of the palladium species (shown in Fig. 4). The 3d core-level lines of **Pd1** fitted with two main peaks, where Pd $3d_{5/2}$ and $3d_{3/2}$ peaks at 342.7 eV and 337.4 eV respectively were assignable to the presence of the Pd(II) species.[11b,23,24] After treatment with bases and substrates in the presence of the **Pd1** catalyst for 4 h, the peaks shifted from 342.7 to 343.0 eV (for Pd $3d_{5/2}$) and from 337.4 eV to 337.8 eV (for Pd $3d_{3/2}$), clearly indicating the presence of Pd(II) species in the reaction mixture.[24] However, the two new peaks at 342.5 eV (for Pd $3d_{5/2}$) and 336.4 eV (for Pd $3d_{3/2}$) indicated the presence of Pd(0) species.[11b,23,24] Hence, we proposed that the Pd(II) complex was converted to some new species containing Pd(0), which was important for catalytic activity. To recognize the species containing Pd(0) we performed FE-SEM and TEM analysis. Electron microscopic data clearly showed the formation of palladium nanoparticles in the solution mixture. From the size distribution curve, the average size of these nanoparticles was estimated to be 3–4 nm (shown in Fig. 5a and b). The SAED pattern revealed the polycrystalline nature of palladium nanoparticles (shown in Fig. 5d). Due to the generation of high surface area Pd(0) exhibited excellent catalytic activity. Hence, this experiment showed that **Pd1** is the pre-catalyst of this catalytic cycle. For obtaining a better insight into the catalytic cycle, we performed the Hg poisoning test. Under optimized reaction conditions, we obtained [1,1′-biphenyl]-4-carbaldehyde as a coupled product in 20% yield after 4 h in the presence of 1 drop of Hg. This reaction confirms that palladium complex **Pd1** is reduced under thermal conditions to

Table 2 Substrate scope for the Pd-catalyzed Suzuki–Miyaura coupling of chlorobenzene derivatives and aryl boronic acids

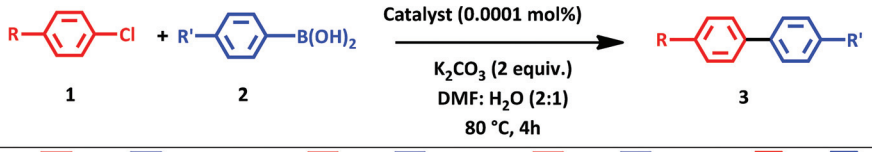

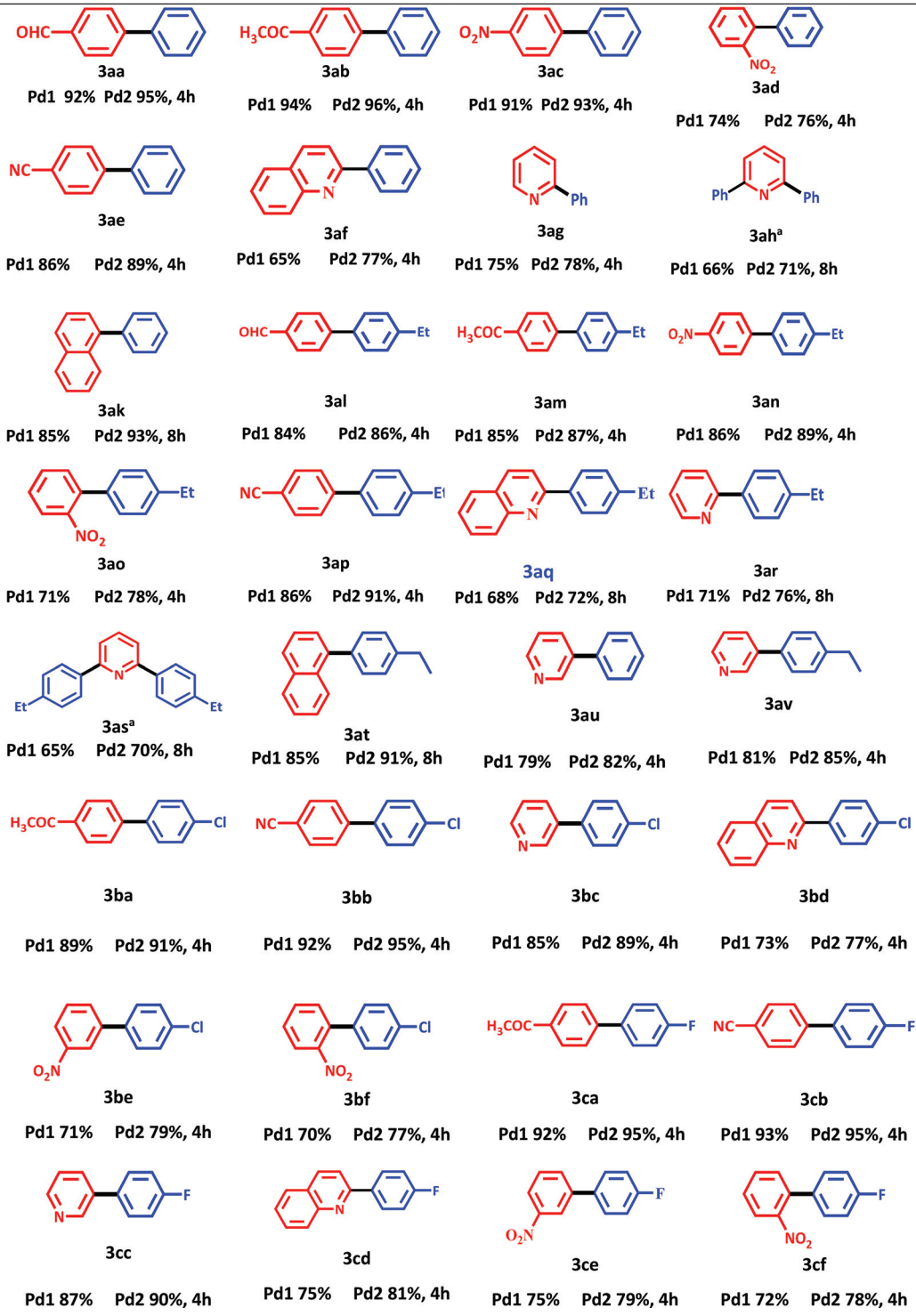

Reaction conditions: **1** (0.0001 mol%), **2a** (1.0 mmol), **3a** (1.2 mmol), base (2 mmol), solvent (4.5 mL), 80 °C, 4–8 h. [a] $PhB(OH)_2$ 2.4 mmol, catalyst loading (0.0002 mol%) and K_2CO_3 4 mmol.

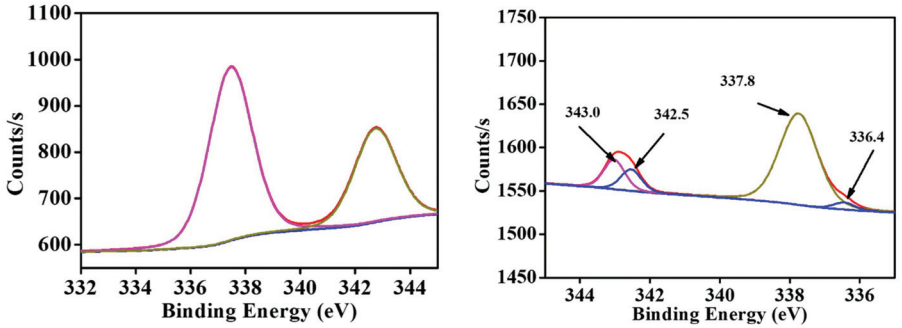

Fig. 4 The XPS spectra of the 3d level of palladium and deconvolution peaks of the Pd species: deconvoluted (red), Pd(II) (magenta and dark yellow), Pd(0) (blue), (a) precatalyst **Pd1** and (b) precatalyst **Pd1** after treatment with K_2CO_3, [1,1′-biphenyl]-4-carbaldehyde and bromobenzene in DMF:H_2O at 80 °C after 4 h.

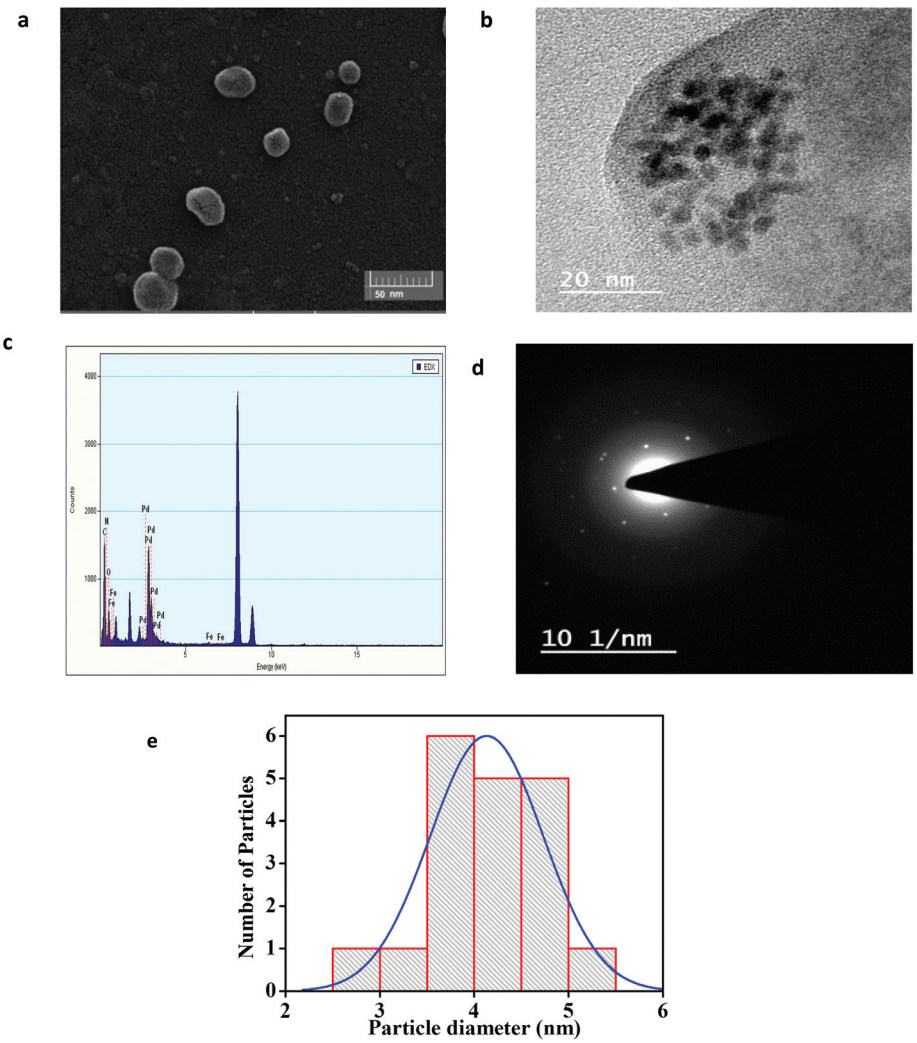

Fig. 5 (a) The SEM image of NPs obtained from catalyst **Pd1**. (b) The TEM image of NPs obtained respectively during SMC (scale bar 50 and 20 nm). (c) EDX analysis of NPs obtained during SMC. (d) The SAED pattern of NPs obtained during SMC. (e) The particle size distribution of spherical Pd nanoparticles obtained during the SMC reaction.

form the palladium(0) species or cluster, followed by oxidative addition of haloarenes to the palladium(0) species.[10e] Then, transmetalation occurs with phenylboronic acid to give rise to intermediate Pd(II). Then, reductive elimination gives rise to the coupled product and regenerates the active species (Scheme 3).[9,20]

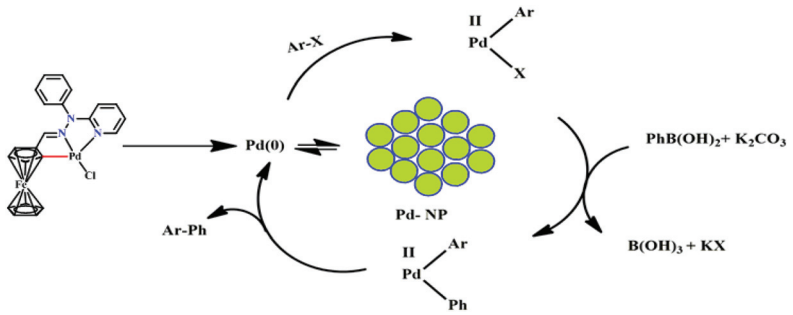

Scheme 3 The proposed catalytic cycle.

Palladium-catalyzed direct C–H arylation reaction under aerobic conditions

Arylated thiazoles and isoxazoles are known to exhibit a variety of interesting biological properties[25] and they can be synthesized *via* the transition metal-catalyzed arylation of thiazoles or isoxazoles with aryl halides. Thus, the reaction of thiazole and bromobenzene was studied and the reaction conditions such as catalyst loading, temperature, reaction time, and base were optimized (Scheme 4 and Fig. 6). The reaction was performed in the presence of various concentrations of palladium catalyst **Pd1**, and it was found that the 0.1 mol% catalyst was efficient to complete the transformation of 4-methylthiazole. Lowering the catalyst loading to 0.02% and 0.05% led to a decrease in the conversion of 4-methylthiazole. This reaction was also screened at various temperatures, revealing that the performance of the catalyst was best in the temperature range of 140–160 °C (shown in Fig. 6).

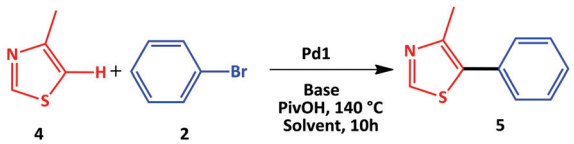

Scheme 4 Screening of reaction conditions for the direct arylation reaction of 4-methylthiazole with bromobenzene.

After the optimization of catalyst loading and temperature, the catalytic reaction was monitored at different time intervals in the presence of bases. From these studies, screening the

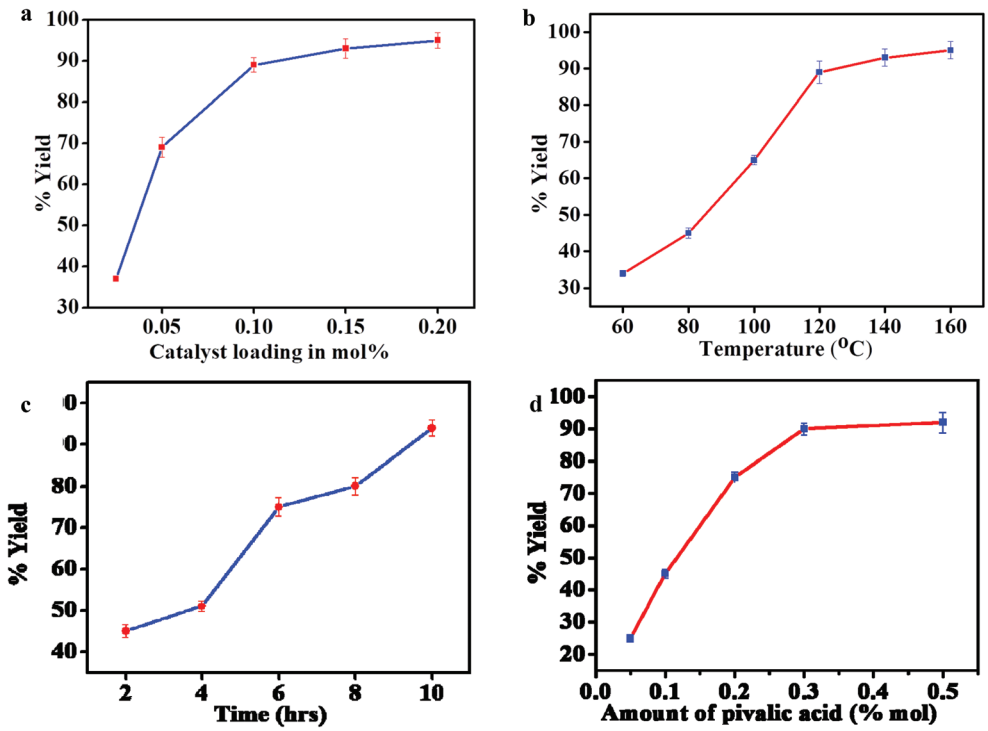

Fig. 6 The reaction profile of palladium-catalyzed (**Pd1**) direct arylation of 4-methylthiazole with aryl bromides. (a) The effect of catalyst loading. (b) The effect of temperature. (c) The effect of time. (d) The effect of the amount of pivalic acid. All the optimization reactions are done three times.

effect of bases on this reaction revealed that KF, Na^{t}OBu, K^{t}OBu and KOAc were inefficient and led to lower conversion of 4-methylthiazole. The use of bases such as $NaHCO_3$ and K_3PO_4 resulted in better conversion of 4-methylthiazole and higher conversion was observed in the case of K_2CO_3 and Na_2CO_3 (Table S7†). This reaction was also investigated with various solvents in the presence of catalyst **Pd1** (Table S7†), which revealed that the use of dimethylacetamide (DMA) as a solvent led to the formation of the product in 94% yield. Control experiments showed that no product was obtained in the absence of catalyst **Pd1** or in the presence of only a ligand and a base (Table S7,† entry 16). Other palladium sources like Na_2PdCl_4 also failed to produce alkylated products under the optimized conditions (Table S7,† entry 17). However, low conversion occurs in the absence of PivOH acid (Table S7,† entry 18).

Several other halides were reacted under these optimized conditions. Substituted bromobenzene reacted smoothly resulting in the arylation of 4-methylthiazole in very good yields. It was observed that aryl halides with different functional groups such as chloro, fluoro, acetyl, cyano, aldehyde and nitro gave excellent yields of 88–95% (shown in Table 3, **6b–6d**, **6g**, **6k**, and **6l**). Substrates with electron-donating groups formed the desired coupled products in moderate yields of up to 75–81% (shown in Table 3, **6b–6d**, **6g**, **6k**, and **6l**). Heteroaryl bromide 3-bromopyridine also resulted in 88–92% yield (Table 3, **6h**) when **Pd1** and **Pd2** were used as catalysts. Sterically hindered 1-naphthyl bromide resulted in a yield of 86% to 92% (Table 3, **6m**). In the case of *meta*-electron-donating haloarene the yield was 70% to 75% (Table 3, **6i**); however, in the case of *meta*-nitro bromobenzene a better yield of 75% to 81% was achieved (Table 3, **6j**). This is due to the steric influence and electronic effects. The catalytic performances of **Pd1** and **Pd2** are comparable, but **Pd2** gives rise to better yields due to the flexibility of the methylene ($-CH_2-$) group. The catalytic efficiencies of **Pd1** and **Pd2** were compared with palladium(II) complexes described previously. Liu and coworkers reported camphyl-based α-diimine palladium complexes for the arylation of thiazoles at 2 mol% loading, which is greater than those of **Pd1** and **Pd2**.[26] Recently the same group has synthesized bulky bis(imino)acenaphthene (BIAN)-supported Pd PEPPSI complexes for the direct arylation of azoles, which are comparable with **Pd1** and **Pd2**.[27]

Table 3 The palladium-catalyzed direct arylation of 4-methylthiazole with aryl bromides

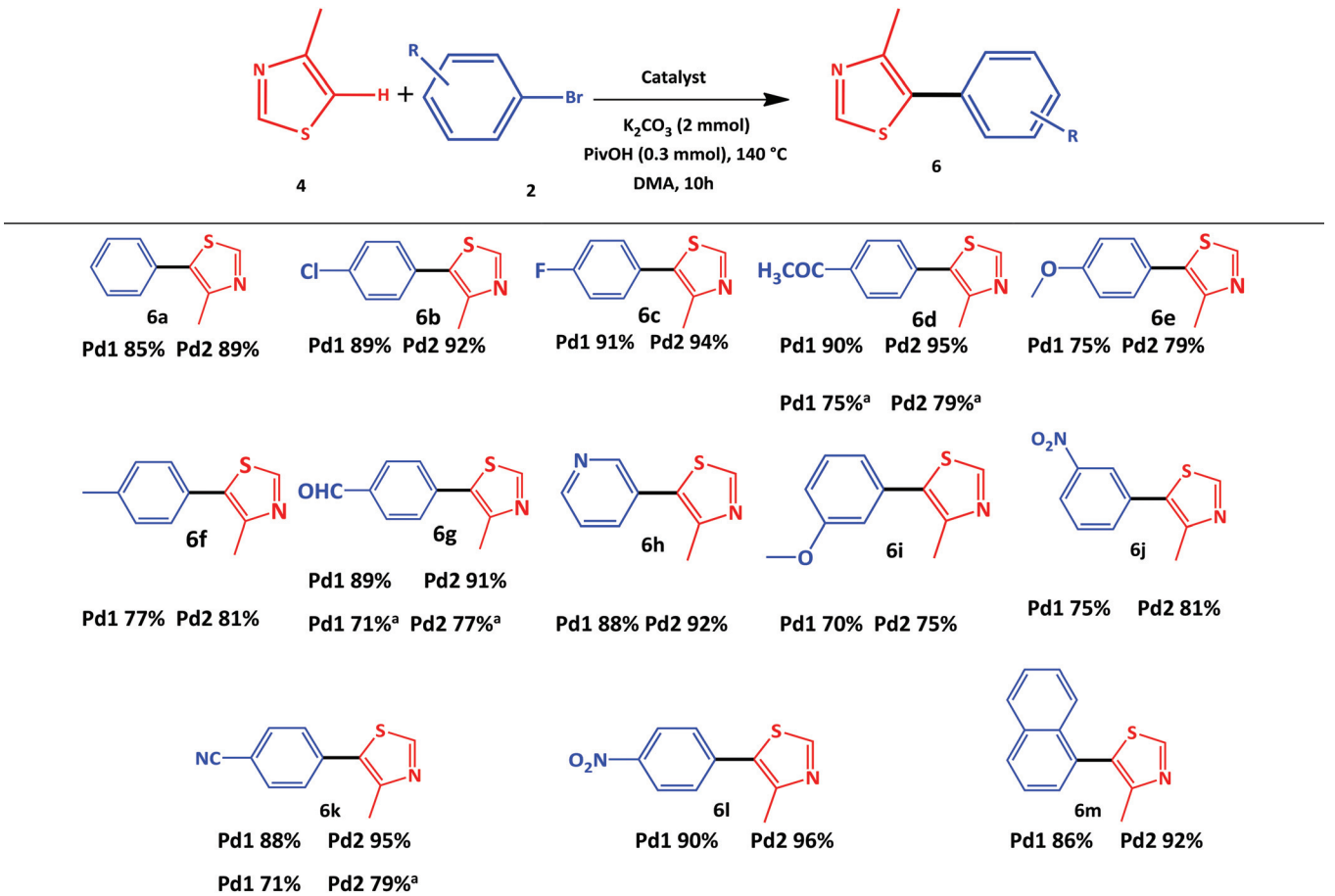

Reaction conditions: Arene (1.2 mmol), aryl bromide (1 mmol), palladium complexes (0.1 mol%), PivOH (0.3 mmol), K_2CO_3 (2 mmol) and DMA (2 mL), 140 °C for 10 h in an aerobic environment. [a] Instead of 4-bromobenzaldehyde, 4-bromo acetophenone and 4-bromobenzonitrile, reaction was done with 4-chlorobenzaldehyde, 4-chloroacetophenone and 4-chlorobenzonitrile respectively, catalyst loading 0.2 mol%.

Other heterocycles like isoxazole derivatives also reacted efficiently with electron-donating and electron-deficient bromides to give the corresponding coupling products. Sterically hindered 3,5-dimethylisoxazole could be coupled efficiently with chloro, aldehyde, fluoro, acetyl, cyano, and nitro groups which gave excellent yields of 78% to 91%. Sterically hindered 1-naphthyl bromide resulted in yields of 79% to 85% (Table 4). Doucet and co-workers established the ligand-free arylation of 3,5-dimethylisoxazole with a catalyst loading of 0.1 mol% to 0.001 mol% which is comparable to **Pd1** and **Pd2**.[28,29] Liu and co-workers reported palladium complexes as catalysts for arylation of sterically hindered 3,5-dimethylisoxazole at 0.1 mol% loading, which is comparable with **Pd1** and **Pd2**.[27,30]

Probable mechanism

The reaction pathway was monitored by X-ray photoelectron spectroscopic (XPS) analysis. After treatment with the base and the substrate in the presence of **Pd1**, for 8 h, we performed XPS analysis which showed that the major Pd $3d_{5/2}$ peak shifted to a binding energy of 342.8 eV and the $3d_{3/2}$ peak shifted to 337.7 eV which were assigned to other Pd(II) species. In addition, two new peaks appeared at 341.8 eV and 336.5 eV which were assigned to Pd $3d_{5/2}$ and Pd $3d_{3/2}$ respectively of the Pd(0)[11b,23,24] species (shown in Fig. 7). These peaks confirm that both Pd(II) and Pd(0) species are present during the catalytic cycle similar to our results obtained during the SMC reaction described previously. We next performed the TEM analysis of the reaction mixture of arylation of 4-methylthiazole. The generation of palladium nanoparticles was observed in the reaction (Fig. 8). The average size of these nanoparticles was estimated to be 10–12 nm. The SAED pattern of the reaction

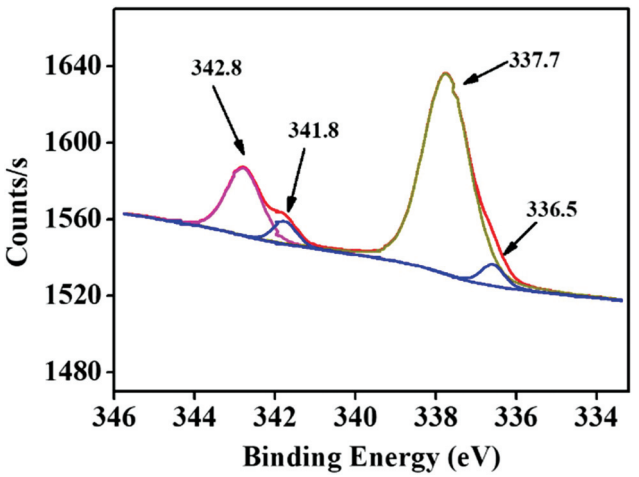

Fig. 7 The XPS spectra of the Pd 3d level and deconvolution peaks of the Pd species: experimental deconvoluted (red), Pd(II) (magenta and dark yellow), and Pd(0) (blue) precatalyst **Pd1** after treatment with K_2CO_3, 4-methylthiazole and bromobenzene in DMA at 140 °C for 8 h.

Table 4 The palladium-catalyzed direct arylation of 3,5-dimethylisoxazole with aryl bromides

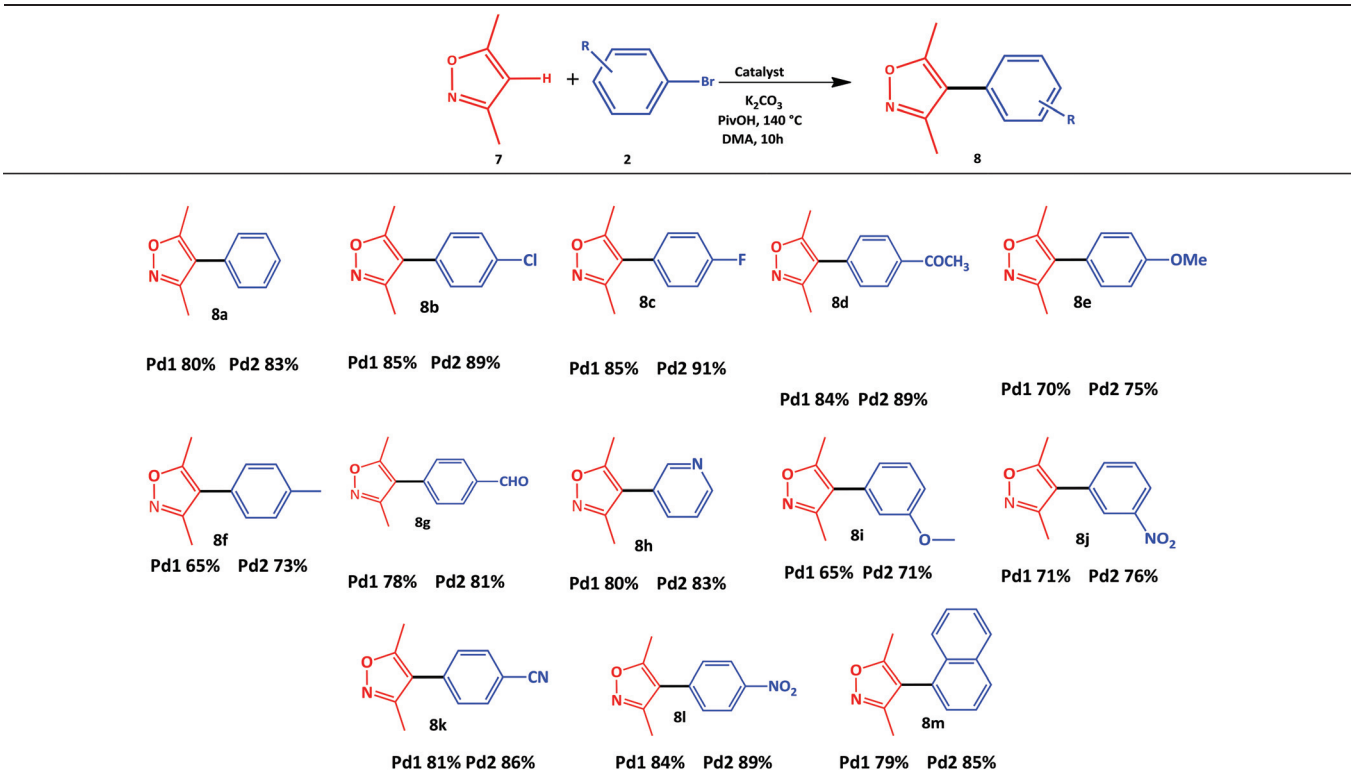

Reaction conditions: Arene (1.2 mmol), aryl bromide (1 mmol), palladium complex (0.1 mol%), PivOH (0.3 mmol), K_2CO_3 (2 mmol) and DMA (2 mL), 140 °C for 10 h in an aerobic environment.

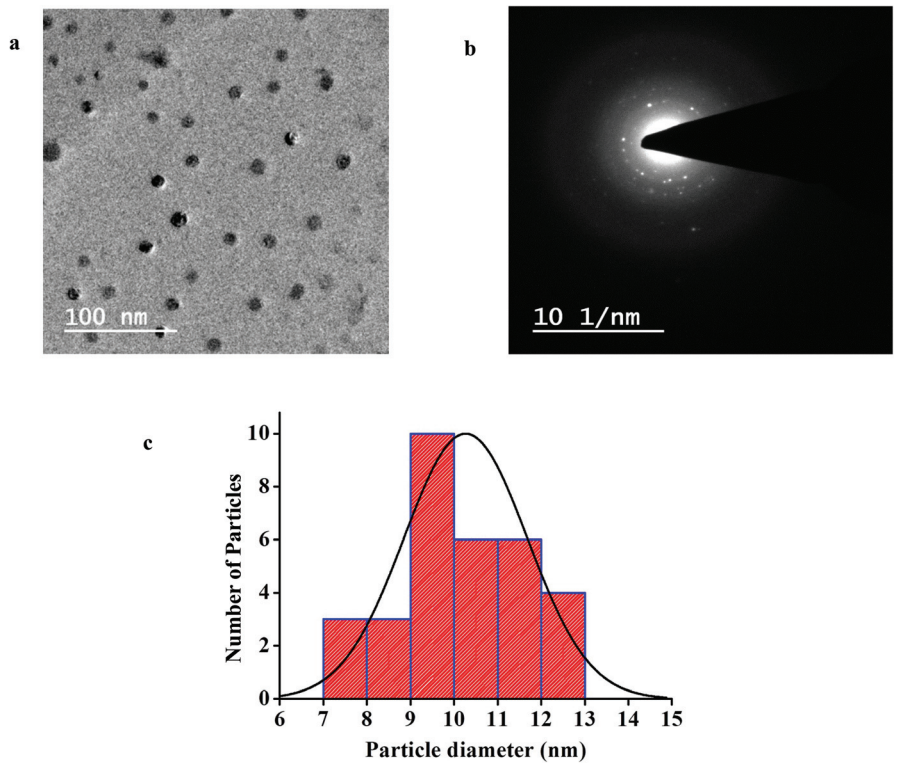

Fig. 8 (a) The TEM image of NPs obtained during arylation of 4-methylthiazole (scale bar 100 nm). (b) The SAED pattern of NPs obtained during arylation of 4-methylthiazole. (c) The particle size distribution of spherical Pd nanoparticles obtained during arylation of 4-methylthiazole.

mixture of arylation of 4-methylthiazole shows the polycrystalline nature of palladium nanoparticles. Based on the data obtained from XPS and TEM analysis, we speculate on the probable reaction pathway for the direct arylation of thiazoles and oxazoles. These experimental results showed that complex **Pd1** is not the actual catalytically active species in this reaction. Palladium complex **Pd1** under thermal conditions form the palladium(0) species or palladium(0) clusters in equilibrium.[15a] Due to the *in situ* formation of the Pd(0) species or the Pd(0) cluster and the high surface area, **Pd1** shows excellent catalytic activity. The oxidative addition of haloarenes gives rise to intermediate **II**. Then ligand exchange occurs with potassium salts of pivalic acid to give intermediate **III**. The C–H bond cleavage step of 4-methylthiazole using pivalate generates intermediate **IV** *via* the CMD transition state,[16a,30,31] which undergoes reductive elimination furnishing the arylated product and regenerating the Pd(0) intermediate (**I**) (Scheme 5).

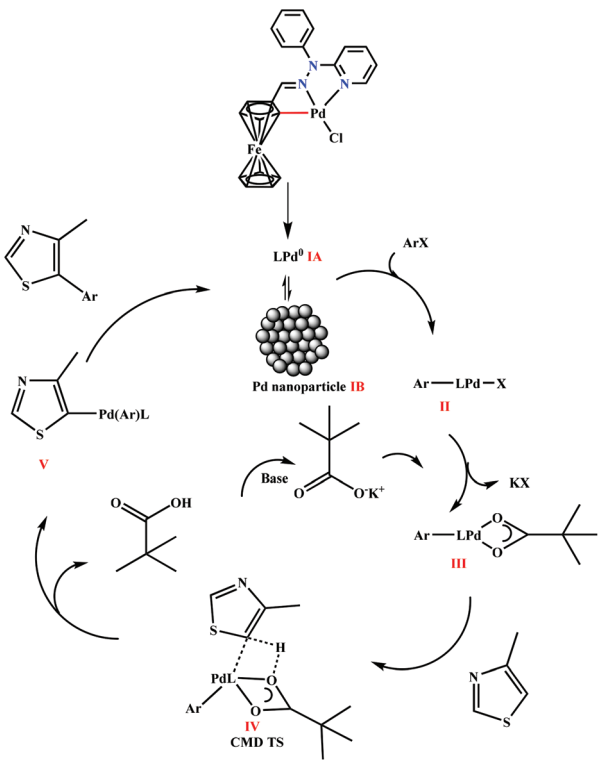

Scheme 5 The proposed catalytic cycle.

Homogeneous and heterogeneous tests

The SMC reaction of 4-chlorobenzaldehyde with phenylboronic acid using catalyst **Pd1** in the presence of mercury and PPh_3 under optimum conditions gives rise to 20% and 37% converted products.

The direct C–H arylation reaction of 4-methylthiazole with bromobenzene catalyzed by **Pd1** in the presence of mercury

and PPh_3 under optimum conditions produces cross-coupled products in 17% and 31% yields. These results show the possibility of the existence of homogeneous Pd(0) species.[22] Furthermore, to establish the nature of the catalysts, hot filtration experiments were performed. In the case of the SMC reaction under standard conditions in the presence of **Pd1** after 1 h, the reaction mixture was filtered. Then the filtrate (reaction mixture) was further continuously stirred under the same reaction conditions. After 4 h the maximum conversion dropped from 94% (4 h) (standard conditions) to 63% (4 h). This experiment showed that some of the palladium was leached from *in situ* generated NPs. These results suggest that the catalytic process is essentially homogeneous.[10d,11b] The direct arylation of 4-methylthiazole with bromobenzene in the presence of **Pd1** under standard conditions resulted in a decrease in conversion from 80% to 59% (standard conditions). These results suggest that the catalytic process is essentially homogeneous.

Conclusions

In summary, we have successfully synthesized and characterized ferrocenyl Schiff bases and organometallic palladium complexes **Pd1** and **Pd2**. The molecular structures of **Pd1** and **Pd2** were authenticated by single crystal X-ray diffraction. Air and moisture-stable complexes **Pd1** and **Pd2** effectively catalyzed the Suzuki–Miyaura cross-coupling reaction with a TON of up to 95×10^4. Investigation of the mechanism indicated that the palladium complexes acted as pre-catalysts and generation of Pd(0) nanoparticles was proposed; Pd(0) nanoparticles were characterized by XPS, SEM, and TEM analysis. Complexes **Pd1** and **Pd2** were found to be efficient catalysts for direct regioselective C_{sp^2}–H functionalization reactions between different heteroarenes (4-methylthiazole and 3,5-dimethylisoxazole) and aryl halides under aerobic conditions with a TON of up to 9.6×10^2. These reactions showed excellent functional group tolerance and a wide range of aryl bromides and various azoles were utilized. The generated Pd(0) nanoparticles were also found to be the active catalyst in these reactions; however, their size and shape were different from our previous results obtained for Suzuki–Miyaura cross-coupling reactions. Studies on other catalytic activities of these interesting organometallic palladium complexes are under progress.

Experimental

The reported methods were used for the synthesis of 2-pyridyl phenylhydrazine[18] and 2-picolylphenylhydrazine.[19] Aryl bromides and chlorides, phenylboronic acids, and K_2CO_3 were procured from Avra, TCI Chemicals (India) Pvt. Ltd. Ferrocenecarboxaldehyde was purchased from Sigma-Aldrich (USA). Solvents used for spectroscopic studies were of HPLC grade and purified by standard procedures before use. Palladium chloride was obtained from Arora Matthey, Kolkata, India. Infrared spectra were recorded as KBr pellets on a Nicolet NEXUS Agilent 1100 FT-IR spectrometer, using 50 scans, and the frequencies were reported in cm^{-1}. Electronic spectra were recorded in CH_2Cl_2 and CH_3OH with an Evolution 600, Thermo Scientific UV-visible spectrophotometer using cuvettes of 1 cm path length. A field emission scanning electron microscope (MIRA3 TESCAN, USA) at an accelerating voltage of 3–10 kV was used for the morphological characterization of the catalytically active species. Transmission electron microscopy (TEM, Tecnai G2 20SeTWIN, FEI Netherlands) was used for the morphological characterization of the catalytically active species. An X-ray photoelectron spectrophotometer (XPS; ULVAC – PHI, INC, Japan) was used for oxidation state calculations and surface morphology determination. ^{1}H-NMR and ^{13}C-NMR spectra were recorded with a Bruker AVANCE 500.13 MHz spectrometer and a JEOL 400 MHz spectrometer, and chemical shifts were reported in δ (ppm) units relative to tetramethylsilane (TMS) as the internal standard. Proton coupling patterns are described as singlet (s), doublet (d), triplet (t), quartet (q), multiplet (m), and broad (br). ESI-MS experiments were performed on a Brüker micrOTOFTM-Q-II mass spectrometer.

X-ray crystallography

Yellow crystals of **Pd1** and **Pd2** were obtained by slow evaporation of solutions of the complexes in acetonitrile. X-ray data collection and processing for complexes were performed on a Bruker Kappa Apex-II CCD diffractometer by using graphite monochromatic Mo-Kα radiation (λ = 0.71073 Å) at 296 K for **Pd1** and at 293 K for **Pd2**. Crystal structures were solved by direct methods. Structure solutions, refinement and data output were carried out with the SHELXTL program.[32–34] All non-hydrogen atoms were refined anisotropically. Hydrogen atoms were placed in geometrically calculated positions and refined using a riding model. Images were created with the DIAMOND program.[35]

Synthetic procedures

Synthesis of L^1H. A methanolic (10 mL) solution of 2-pyridyl phenylhydrazine (0.370 g, 2.0 mmol) was placed in a 50 mL round bottom flask and stirred at room temperature for 5 min. Ferrocene carboxaldehyde (0.428 g, 2.0 mmol), also dissolved in methanol (10 mL), was added dropwise with stirring. Then the reaction mixture was stirred for another 3 h. A red color solid was filtered off and washed with cold methanol. Yield: 585 mg 77% ($\mathbf{L^1H}$).

Selected IR data: (KBr, ν/cm^{-1}): 1585 ($\nu_{C=N}$) UV-visible [CH_2Cl_2, λ_{max}/nm (ε/M^{-1} cm^{-1})]: 484(3950), 335(22 850), 290 (20 850), 255(23 950). Anal. calcd for $C_{22}H_{19}FeN_3$: C, 69.31; H, 5.02; N, 11.02; found: C, 69.13; H, 5.12; N, 11.15. ^{1}H-NMR (400 MHz, δ/ppm, $CDCl_3$): 8.10 (d, J = 4.7, 1H); 7.61 (t, J = 3.9, 8.0 Hz, 4H); 7.47 (t, J = 7.4 Hz, 1H); 7.24 (s, 2H); 7.07 (s, 1H); 6.75–6.72 (m, 1H), 4.55 (s, 2H), 4.30 (s, 2H), 4.11 (s, 5H). ^{13}C-NMR (400 MHz, δ/ppm, $CDCl_3$): 158.5; 147.6; 139.4; 138.5; 137.5; 130.5; 129.9; 128.4; 115.3; 109.5; 81.1; 69.6; 69.1; 67.1. ESI-MS (CH_3CN): m/z = 382.0305 for the $[\mathbf{L^1H}]^+$ ion.

Synthesis of L^2H. A methanolic (10 mL) solution of 2-picolylphenylhydrazine (0.370 g, 2 mmol) was placed in a 50 mL round bottom flask and stirred at room temperature for 5 min. Ferrocene carboxaldehyde (0.428 g, 2.0 mmol), also dissolved in methanol (10 mL), was added dropwise with stirring. Then the reaction mixture was stirred for another 3 h. A red color solid was filtered off and washed with cold methanol. Yield: 596 mg 75% (L^2H). Selected IR data: (KBr, ν/cm^{-1}): 1594 ($\nu_{C=N}$) UV-visible [CH_2Cl_2, λ_{max}/nm (ε/M^{-1} cm^{-1})]: 439(1588), 324(29 530), 252(17 540). Anal. calcd for $C_{23}H_{21}FeN_3$: C, 69.89; H, 5.35; N, 10.63; found: C, 69.73; H, 5.47; N, 10.57. ^{1}H-NMR (400 MHz, δ/ppm, $CDCl_3$): 8.67 (d, J = 4.5, 1H); 7.63 (t, J = 7.6, 9.2 Hz, 1H); 7.36–7.29 (m, 4H); 7.23 (s, 2H); 7.15 (d, J = 7.8 Hz, 1H); 6.93 (t, J = 8.0, 6.6, 1H), 5.22 (s, 2H), 4.55 (s, 2H), 4.25 (s, 2H), 3.99 (s, 5H). ^{13}C-NMR (400 MHz, δ/ppm, $CDCl_3$): 156.6; 149.8; 147.6; 137.0; 132.9; 129.1; 122.4; 120.7; 120.2; 114.2; 82.0; 69.1; 68.9; 67.7; 51.9(–CH_2–). ESI-MS (CH_3CN): m/z = 395.1137 for the $[L^2H]^+$ ion.

Syntheses of complexes Pd1 and Pd2

0.10 mmol ligand (L^1H: 0.038 g and L^2H: 0.039 g) was stirred in 40 mL of methanol for 15 min. $Na_2[PdCl_4]$ (0.029 g, 0.10 mmol) was added to it. The mixture was stirred further for 6 h at 60 °C. The red solid formed was collected by filtration and air-dried overnight to obtain complexes **Pd1** and **Pd2**.

The single crystals of each of the two complexes were obtained from a mixture of dichloromethane : methanol (1 : 3).

Complex Pd1. Yield: 35 mg 67%, Selected IR data: (KBr, ν/cm^{-1}): 1620 ($\nu_{C=N}$) UV-visible [CH_2Cl_2, λ_{max}/nm (ε/M^{-1} cm^{-1})]: 529(2250), 371(5530), 285(14 420), 239(17 710). Anal. calcd for $C_{22}H_{18}ClFeN_3Pd$: C, 50.61; H, 3.47; N, 8.05; found: C, 50.67; H, 3.35; N, 8.23. ^{1}H-NMR (400 MHz, δ/ppm, DMSO): 7.18 (s, 1H); 6.79–6.72 (m, 4H); 6.66 (d, J = 5.8, 2H); 6.10 (s, 1H); 6.05 (t, J = 5.0, 4.8, 1H); 3.48 (s, 1H); 3.36 (d, J = 8.5, 2H); 3.30 (s, 5H). ^{13}C-NMR (400 MHz, δ/ppm, DMSO): 157.7; 140.9; 135.2; 132.1; 131.7; 130.2; 117.2; 115.0; 109.8; 90.73; 74.9; 70.76; 68.14; 67.8. ESI-MS (CH_3CN): 527.0384 for the [**Pd1** + CH_3CN–Cl]$^+$ ion.

Complex Pd2. Yield: 41 mg 76%, Selected IR data: (KBr, ν/cm^{-1}): 1603 ($\nu_{C=N}$) UV-visible [CH_2Cl_2, λ_{max}/nm (ε/M^{-1} cm^{-1})]: 532(1460), 359(2620), 272(16 060), 244(21 800). Anal. calcd for $C_{23}H_{20}ClFeN_3Pd$: C, 51.52; H, 3.76; N, 7.84; found: C, 51.41; H, 3.69; N, 7.97. ^{1}H-NMR (400 MHz, δ/ppm, DMSO): δ 9.05 (d, J = 4.9 Hz, 1H), 8.72 (s, 1H), 7.91 (t, J = 8.4 Hz, 1H), 7.66 (d, J = 7.4 Hz, 1H), 7.43 (d, J = 7.0 Hz, 1H), 7.18 (t, J = 7.5 Hz, 2H), 7.11 (s, 2H), 6.84 (t, J = 7.0 Hz, 1H), 5.75 (s, 2H), 4.86 (s, 1H), 4.60 (s, 1H), 4.56 (s, 1H), 4.38 (s, 5H). ESI-MS (CH_3CN): 534.9662 for the [**Pd2** + H$^-$]$^+$ ion.

General procedure for the SMC reaction

The Pd(II) complex (0.0001 mol%) in DMF (3 mL) was added to a mixture of chloro substituted benzene (1.0 mmol), aryl boronic acid (1.2 mmol), and K_2CO_3 (2 mmol) in H_2O (1.5 mL) taken in a 20 mL round bottom flask. After stirring for 4–8 h at 80 °C, the reaction mixture was cooled and quenched by adding 20 mL of water. The mixture was extracted with ethyl acetate (2 × 10 mL). The combined extract was washed with water and dried over anhydrous Na_2SO_4. The solvent of the extract was removed under reduced pressure with a rotary evaporator to obtain the product. The crude products were purified by column chromatography on silica gel using hexane/ethyl acetate as an eluent. The isolated cross-coupled products were authenticated by ^{1}H- and ^{13}C-NMR spectra displayed in Fig. S22–S85 in the ESI.†

General procedure for the arylation reaction

An oven-dried flask (10 mL) was charged with 4-methylthiazole (1.2 mmol) or 3,5-dimethylisoxazole (1.2 mmol), an aryl halide (1.0 mmol), a base (2.0 mmol), an acid additive (0.30 mmol), a catalyst (0.1 mol%) and 2 mL of solvent. The flask was placed in a pre-heated oil bath at 140 °C under aerobic conditions, and the reaction mixture was stirred. After completion of the reaction, the mixture was cooled to room temperature and quenched by adding 10 mL of water. This mixture was extracted with dichloromethane (3 × 15 mL). The combined organic layer was washed with water and dried over anhydrous Na_2SO_4. The solvent of the extract was removed under reduced pressure with a rotary evaporator to obtain the product. The crude products were purified by column chromatography on silica gel using hexane/ethyl acetate as an eluent. The isolated cross-coupled products were authenticated by ^{1}H and ^{13}C NMR spectra displayed in Fig. S86–S137 in the ESI.† GC-MS mass spectra of some respective direct arylation products are shown in Fig. S138–S141.†

XPS analysis. The sample for XPS analysis was prepared as follows: after the Suzuki–Miyaura reaction of 4-chlorobenzaldehye with phenylboronic acid in the presence of **Pd1** under optimized conditions, the reaction mixture was dropped onto a glass slide. Then the sample was dried under air. The resulting sample was then used for XPS analysis.

FE-SEM and TEM analyses. The sample for TEM analysis was prepared as follows: after the Suzuki–Miyaura reaction of 4-chlorobenzaldehye with phenylboronic acid in the presence of **Pd1**, the reaction mixture was diluted with DMF and water. Then one drop was dropped onto a copper grid. Then the sample was dried under air. The resulting sample was then used for TEM analysis. For FE-SEM the same technique was followed except that instead of the copper grid, the sample was prepared on a glass slide. The same process was also followed for the sample preparation from direct C–H arylation reaction catalyzed by **Pd1** for TEM analysis.

Hg poisoning test. To carry out the Hg poisoning test, catalyst **Pd1** (0.0001 mol%) was stirred with 1 drop of Hg in an oven-dried RB flask. After that, 4-chlorobenzaldehyde (1.0 mmol), phenylboronic acid (1.2 mmol) and K_2CO_3 (2 mmol) were added to the flask and the reaction was carried out under optimum conditions. Reaction progress was monitored by TLC. The reaction was further continued for 4 hours at 80 °C. The same procedure was followed for direct C–H arylation reaction catalyzed by **Pd1**, with 4-methylthiazole (1.2 mmol), an aryl halide (1.0 mmol), K_2CO_3 (2.0 mmol), an acid additive (0.30 mmol), catalyst **Pd1** (0.1 mol%) and 3 mL of

solvent at 140 °C. After standard workup of the reaction mixture, % yield was determined using ^{1}H-NMR.

PPh_3 poisoning test. In an oven-dried RB flask, catalyst **Pd1** (0.0001 mol%) was stirred with PPh_3 (5 mol%), 4-chlorobenzaldehyde (1.0 mmol), phenylboronic acid (1.2 mmol) and K_2CO_3 (2 mmol) and the reaction was carried out under optimum conditions. Reaction progress was monitored by TLC. The reaction was further continued for 4 hours at 80 °C. The same procedure was followed for direct C–H arylation reaction catalyzed by **Pd1**, with 4-methylthiazole (1.2 mmol), an aryl halide (1.0 mmol), K_2CO_3 (2.0 mmol), an acid additive (0.30 mmol), catalyst **Pd1** (0.1 mol%) and 3 mL of solvent at 140 °C. Then 5 mol% PPh_3 was added and the reaction was carried out for 10 h under optimum conditions. After standard workup of the reaction mixture, % yield was determined using ^{1}H-NMR.

Conflicts of interest

There are no conflicts to declare.

Acknowledgements

KG thanks the of Scientific and Industrial Research, India, New Delhi (01(2942)/18/EMR-II dated 01-05-2018) for financial assistance. Ankur Maji, Anshu Singh, and Aurobinda Mohanty also thank the MHRD for their fellowships. We thank Prof. Marilyn Olmstead for her help in solving crystal structure.

References

1 (*a*) J. Magano and J. R. Dunetz, *Chem. Rev.*, 2011, **111**, 2177; (*b*) D. Astruc, C. Ornelas and J. Ruiz, *Acc. Chem. Res.*, 2008, **41**, 841; (*c*) D. R. Staveren and N. Metzler-Nolte, *Chem. Rev.*, 2004, **104**, 5931; (*d*) E. Hillard, A. Vessires, L. Thouin, G. Jaouen and C. Amatore, *Angew. Chem.*, 2006, **118**, 291.

2 (*a*) A. Singh, I. Lumb, V. Mehra and V. Kumar, *Dalton Trans.*, 2019, **48**, 2840; (*b*) C. Mu, K. E. Prosser, S. Harrypersad, G. A. MacNeil, R. Panchmatia, J. R. Thompson, S. Sinha, J. J. Warren and C. J. Walsby, *Inorg. Chem.*, 2018, **57**, 15247; (*c*) S. González-Pelayo, E. López, J. Borge, N. S. Álvarez and L. A. López, *Molecules*, 2018, **23**, 1335.

3 (*a*) M. Hapke, L. Brandt and A. Lutzen, *Chem. Soc. Rev.*, 2008, **37**, 2782; (*b*) C. Kaes, A. Katz and M. W. Hosseini, *Chem. Rev.*, 2000, **100**, 3553; (*c*) G. Hamasaka, F. Sakurai and Y. Uozumi, *Chem. Commun.*, 2015, **51**, 3886.

4 (*a*) L. X. Dai, T. Tu, S. L. You, W. P. Deng and X. L. Hou, *Acc. Chem. Res.*, 2003, **36**, 659; (*b*) C. Chen, T. M. J. Anselment, R. Frohlich, B. Rieger, G. Kehrand and G. Erker, *Organometallics*, 2011, **30**, 5248; (*c*) M. Sato, H. M. Shigeta and J. Sekino, *J. Organomet. Chem.*, 1993, **458**, 199; (*d*) Z. Weng, S. Teo and T. S. A. Hor, *Acc. Chem. Res.*, 2007, **40**, 676; (*e*) V. I. Sokolov, *Chin. J. Org. Chem.*, 2018, **38**, 75.

5 A. Togni, C. Breutel, A. Schnyder, F. Spindler, H. Landert and A. Tijani, *J. Am. Chem. Soc.*, 1994, **116**, 4062.

6 (*a*) S. Ø. Scottwell, K. J. Shaffer, C. J. McAdam and J. D. Crowley, *RSC Adv.*, 2014, **4**, 35726; (*b*) V. C. Gibson, C. M. Halliwell, N. J. Long, P. J. Oxford, A. M. Smith, A. J. P. White and D. J. Williams, *Dalton Trans.*, 2003, 918.

7 L. A. López and E. López, *Dalton Trans.*, 2015, **44**, 10128.

8 (*a*) T. Shibata and T. Shizuno, *Angew. Chem., Int. Ed.*, 2014, **53**, 5410; (*b*) Z. J. Cai, C. X. Liu, Q. Wang, Q. Gu and S. L. You, *Nat. Commun.*, 2019, **10**, 4168; (*c*) K. Plevova, B. Mudrakova, E. Rakovsky and R. Sebesta, *J. Org. Chem.*, 2019, **84**, 7312; (*d*) M. Sattar, Praveen, C. D. Prasad, A. Verma, S. Kumar and S. Kumar, *Adv. Synth. Catal.*, 2016, **358**, 240.

9 R. Martin and S. L. Buchwald, *Acc. Chem. Res.*, 2008, **41**, 1461.

10 (*a*) Q. Luo, J. Tan, Z. Li, W. Nan and D. J. Xiao, *J. Org. Chem.*, 2012, **77**, 8332; (*b*) G. Hamasaka, S. Ichii and Y. A. Uozumi, *Adv. Synth. Catal.*, 2018, **360**, 1833; (*c*) D. Roy and Y. Uozumi, *Adv. Synth. Catal.*, 2018, **360**, 602; (*d*) M. T. Reetza and J. G. de Vries, *Chem. Commun.*, 2004, 1559; (*e*) J. G. de Vries, *Dalton Trans.*, 2006, 421.

11 (*a*) F. X. Roca and C. J. A. Richards, *Chem. Commun.*, 2003, 3002; (*b*) H. Liu, T. Li, X. Xue, W. Xu and Y. Wu, *Catal. Sci. Technol.*, 2016, **6**, 1667; (*c*) Z. Fu, T. Li, X. He, J. Liu and Y. Wu, *RSC Adv.*, 2014, **4**, 26413.

12 (*a*) S. Kumar, G. K. Rao, A. Kumar, M. P. Singh and A. K. Singh, *Dalton Trans.*, 2013, **42**, 16939; (*b*) X. Li, X. Zhao, J. Zhang and Y. Zhao, *Chem. Commun.*, 2013, **49**, 10004; (*c*) L. Liu, Y. Dong and N. Tang, *Green Chem.*, 2014, **16**, 2185; (*d*) L. Yin and J. Liebscher, *Chem. Rev.*, 2007, **107**, 133; (*e*) V. Arumugam, W. Kaminsky, N. S. P. Bhuvanesh and D. Nallasamy, *RSC Adv.*, 2015, **5**, 59428; (*f*) F. S. Han, *Chem. Soc. Rev.*, 2013, **42**, 5270; (*g*) Y. Tsuji and T. Fujihara, *Inorg. Chem.*, 2007, **46**, 1895; (*h*) V. V. Grushin and H. Alper, *Chem. Rev.*, 1994, **94**, 1047.

13 (*a*) L. Ackermann, R. Vicente and A. R. Kapdi, *Angew. Chem., Int. Ed.*, 2009, **48**, 9792; (*b*) J. Roger, A. L. Gottumukkala and H. Doucet, *ChemCatChem*, 2010, **2**, 20; (*c*) I. V. Seregin and V. Gevorgyan, *Chem. Soc. Rev.*, 2007, **36**, 1173; (*d*) C. B. Bheeter, L. Chen, J.-F. Soulé and H. Doucet, *Catal. Sci. Technol.*, 2016, **6**, 2005.

14 (*a*) D. S. Hewings, M. Wang, M. Philpott, O. Fedorov, S. Uttarkar, P. Filippakopoulos, S. Picaud, C. Vuppusetty, B. Marsden, S. Knapp, S. J. Conway and T. D. Heightman, *J. Med. Chem.*, 2011, **54**, 6761; (*b*) C. Galdeano, M. S. Gadd, P. Soares, S. Scaffidi, I. Van Molle, I. Birced, S. Hewitt, D. M. Dias and A. Ciulli, *J. Med. Chem.*, 2014, **57**, 8657; (*c*) Y. Katsura, S. Nishino, Y. Inoue, K. Sakane, Y. Matsumoto, C. Morinaga, H. Ishikawa and H. Takasugi, *J. Med. Chem.*, 2002, **45**, 143.

15 (*a*) M. Ye, G. L. Gao, A. J. F. Edmunds, P. A. Worthington, J. A. Morris and J. Q. Yu, *J. Am. Chem. Soc.*, 2011, **133**, 19090; (*b*) R. Takita, D. Fujita and F. Ozawa, *Synlett*, 2011, 959; (*c*) S. Tani, T. N. Uehara, J. Yamaguchi and K. Itami, *Chem. Sci.*, 2014, **5**, 123.

16 (*a*) A. Feyrer and F. Breher, *Inorg. Chem. Front.*, 2017, **4**, 1125; (*b*) A. K. Sharma, H. Joshi, R. Bhaskar, S. Kumar and A. K. Singh, *Dalton Trans.*, 2017, **46**, 2485.

17 (*a*) V. A. Zinovyeva, M. A. Vorotyntsev, I. Bezverkhyy, D. Chaumont and J. C. Hierso, *Adv. Funct. Mater.*, 2011, **21**, 1064; (*b*) Y. Li, X. Yu, Y. Wang, H. Fu, X. Zheng, H. Chen and R. Li, *Organometallics*, 2018, **37**, 979.

18 K. Ghosh, N. Tyagi, P. Kumar, U. P. Singh and N. Goel, *J. Inorg. Biochem.*, 2010, **104**, 9.

19 (*a*) S. Rathi, A. Maji, O. Singh and K. Ghosh, *J. Indian Chem. Soc.*, 2015, **92**, 1913; (*b*) S. Rathi, A. Maji, U. P. Singh and K. Ghosh, *Inorg. Chim. Acta*, 2019, **486**, 261; (*c*) A. Maji, O. Singh, S. Rathi, U. P. Singh and K. Ghosh, *ChemistrySelect*, 2019, **4**, 7246.

20 L. A. Bulygina, Z. A. Starikova, K. K. Babievskii, I. A. Utepova, V. L. Rusinov, O. N. Chupakhin and V. I. Sokolov, *Russ. Chem. Bull. Int. Ed.*, 2008, **57**, 2214.

21 L. A. Bulygina, N. D. Kagramanov, N. S. Khrushcheva, K. A. Lyssenko, A. S. Peregudov and V. I. Sokolov, *J. Organomet. Chem.*, 2017, **846**, 169.

22 (*a*) V. Sable, K. Maindan, A. R. Kapdi, P. S. Shejwalkar and K. Hara, *ACS Omega*, 2017, **2**, 204; (*b*) G. K. Rao, A. Kumar, S. Kumar, U. B. Dupare and A. K. Singh, *Organometallics*, 2013, **328**, 2452.

23 T. Begum, M. Mondal, M. P. Borpuzari, R. Kar, G. Kalita, P. K. Gogoi and U. Bora, *Dalton Trans.*, 2017, **46**, 539.

24 (*a*) G. Liu, F. Han, C. Liu, H. Wu, Y. Zeng, R. Zhu, X. Yu, S. Rao, G. Huang and J. Wang, *Organometallics*, 2019, **38**, 1459; (*b*) M. T. Finn, C. M. Donahue, A. V. Blake, N. An, S. R. Daly and A. M. Voutchkova-Kostal, *Eur. J. Inorg. Chem.*, 2018, 2471; (*c*) N. Huang, Y. Xu and D. Jiang, *Sci. Rep.*, 2014, **4**, 7228.

25 (*a*) K. B. Sarojini, B. G. Krishna, C. G. Darshanraj, R. B. Bharath and H. Manjunatha, *Eur. J. Med. Chem.*, 2010, **45**, 3490; (*b*) K. Sohda, K. Nagai, T. Yamori, K. Suzuki and A. Tanaka, *J. Antibiot.*, 2005, **58**, 27; (*c*) A. R. Katritzky and C. W. Rees, *Comprehensive Heterocyclic Chemistry*, Pergamon Press, Oxford, 1984, vol. 2; (*d*) A. R. Katritzky, C. W. Rees and E. F. V. Scriven, *Comprehensive Heterocyclic Chemistry II*, Elsvier, Oxford, 1996, vol. 5; (*e*) T. Eicher and S. Hauptmann, *The Chemistry of Heterocycles*, Wiley-VCH, Weinheim, 2nd edn, 2003.

26 F. M. Chen, D. D. Lu, L.-Q. Hu, J. Huang and F. S. Liu, *Org. Biomol. Chem.*, 2017, **15**, 5731.

27 L. Q. Hu, R. L. Deng, Y. F. Li, C. J. Zeng, D. S. Shen and F. S. Liu, *Organometallics*, 2018, **37**, 214.

28 J. Roger, F. Pozgan and H. Doucet, *J. Org. Chem.*, 2009, **74**, 1179.

29 Y. Fall, C. Reynaud, H. Doucet and M. Santelli, *Eur. J. Org. Chem.*, 2009, 4041.

30 F. M. Chen, F. D. Huang, X. Y. Yao, T. Li and F. S. Liu, *Org. Chem. Front.*, 2017, **4**, 2336.

31 (*a*) M. Lafrance and K. Fagnou, *J. Am. Chem. Soc.*, 2006, **128**, 16496; (*b*) I. Gorelsky, D. Lapointe and K. Fagnou, *J. Org. Chem.*, 2012, **77**, 658; (*c*) S. I. Gorelsky, *Coord. Chem. Rev.*, 2013, **257**, 153; (*d*) S. Tani, T. N. Uehara, J. Yamaguchia and K. Itami, *Chem. Sci.*, 2014, **5**, 123.

32 G. M. Sheldrick, *Acta Crystallogr., Sect. A: Found. Crystallogr.*, 1990, **46**, 467.

33 G. M. Sheldrick, *SHELXTL NT 2000 version 6.12, Reference Manual*, University of Gottingen, Pergamon, New York, 1980.

34 O. V. Dolomanov, L. J. Bourhis, R. J. Gildea, J. A. K. Howard and H. Puschmann, *J. Appl. Crystallogr.*, 2009, **42**, 339.

35 B. Klaus, *Diamond, Version 1.2 c*, University of Bonn, Germany, 1999.

